

Al-Mg ISOTOPIC CONSTRAINTS ON THE CONDENSATION AGE OF FINE-GRAINED REFRACTORY INCLUSIONS IN REDUCED CV3 CHONDRITES. J. Han¹, N. Matsuda², M.-C. Liu^{2,3}, C. Park⁴, and L. P. Keller⁵.

¹Department of Earth and Atmospheric Sciences, University of Houston, Houston TX, 77204, USA (jhan28@central.uh.edu), ²Department of Earth, Planetary, and Space Sciences, UCLA, Los Angeles, CA 90095, USA, ³Lawrence Livermore National Laboratory, Livermore, CA 94551, USA, ⁴Division of Earth-System Sciences, Korea Polar Research Institute, 26 Songdomirae-ro, Yeosu-gu, Incheon 21990, South Korea, ⁵ARES, XI3, NASA Johnson Space Center, 2101 NASA Parkway, Houston, TX 77058, USA.

Introduction: Fine-grained Ca-Al-rich inclusions (FGIs) in carbonaceous chondrites are interpreted as aggregates of direct condensates from the solar nebula that escaped extensive melting [1]. Thus far, a few high-precision SIMS Al-Mg chronology studies of FGIs from CV3 chondrites have been reported [2-4]. [2,3] argued that $(^{26}\text{Al}/^{27}\text{Al})_0$ of all FGIs are close to the bulk refractory inclusion value of $\sim 5.2 \times 10^{-5}$ [5,6], which may define a time zero for the FGI condensation. A similar $(^{26}\text{Al}/^{27}\text{Al})_0$ value was also inferred from an amoeboid olivine aggregate (AOA) [7], which also represents a direct condensate from the solar nebula [8]. In contrast, [4] reported significant variations in $(^{26}\text{Al}/^{27}\text{Al})_0$ of FGIs, ranging from $\sim 5.2 \times 10^{-5}$ to $\sim 3.4 \times 10^{-5}$, and concluded that their formation continued over at least ~ 0.4 Ma after the canonical value. These contrasting results suggest that the chronological significance for the formation age spread of FGIs in CV3 chondrites is still poorly constrained.

Building on our preliminary SIMS study [9], we report Al-Mg isotopic data of seven FGIs from reduced CV3 chondrites to better establish the distribution of $(^{26}\text{Al}/^{27}\text{Al})_0$ of FGIs relative to coarse-grained, igneous CAIs (CGIs) in CV3 chondrites [10]. We also analyzed two fluffy Type A CAIs (FTAs), which are widely believed to be the product of nebular condensation [11]. The overall objective of our isotopic study was to provide additional chronological constraints on condensation processes in the early solar nebula.

Methods: Our initial mineralogical and petrologic characterizations of CAIs from reduced CV3 chondrites Efremovka, Thiel Mountains (TIL) 07003, and TIL 07007 were conducted using a FEI Quanta 3D FEG dual beam SEM/FIB and a JEOL JXA-8530F electron microprobe at NASA JSC.

In addition to three FGIs from Efremovka [9], six inclusions from TIL 07003 and TIL 07007 were analyzed in a high-precision multicollection mode on the CAMECA ims-1290 ion microprobe at UCLA. Hibonite, spinel, melilite, and diopside were sputtered with a 2-3 nA $^{16}\text{O}_3^-$ primary ion beam generated by a Hyperion-II oxygen plasma source. Our detailed analytical procedure was described in [12].

Results & Discussion: The six CAIs from TIL 07003 and TIL 07007 studied here include four FGIs and two FTAs. These inclusions usually display a

nodular structure, consistent with a condensation origin [1,11]. However, important variations in mineralogy, modal abundance, and nodule size and shape are observed among them, suggestive of their complex condensation history under non-equilibrium conditions. All CAIs studied here lack Na-rich and Fe-rich phases of likely secondary parent body alteration origin.

TIL 3-02 is a mineralogically uniform FGI, which contains spinel-melilite-rich nodules. These nodules are rimmed successively by a sequence of intimate intergrowths of spinel + Al,Ti-diopside + perovskite, anorthite, diopside, and finally forsterite. TIL 3-05 is a fragment of FGI, consisting of intergrown spinel and melilite. Anorthite appears to partially replace melilite. A diopside rim occurs on the one side of the inclusion. TIL 7-02 is a compound FGI, consisting of two mineralogically distinct units. The first unit is dominated by melilite-cored, diopside-rimmed nodules. The second unit contains melilite-rich nodules, in which the melilite cores are surrounded by a thin layer of intergrown spinel and Al,Ti-diopside below a diopside rim. Spinel also occurs with perovskite as a core in some of larger nodules in this unit. TIL 7-06 is a zoned, melilite-rich FGI. The core contains smaller hibonite-rich nodules with spinel, whereas the mantle is dominated by spinel-cored nodules with perovskite and minor hibonite. The nodules are separated by diopside.

TIL 7-01 is a FTA, consisting of melilite-rich nodules with perovskite and spinel. The individual nodules are rimmed by diopside and forsterite. TIL 7-07 is an elliptical-shaped FTA. The center of the largest nodule consists mainly of melilite with Al,Ti-diopside + anorthite bands. Spinel occurs throughout the inclusion, but larger grains are concentrated towards a diopside rim and in nodules on the outer region of the inclusion.

Overall, the observed mineralogical and textural characteristics from individual FGIs and FTAs indicate that these inclusions represent primary condensates that had not been melted after their initial formation [1,11]. Therefore, the FGIs and FTAs studied here likely preserve Al-Mg isotopic compositions at the time of their formation by condensation in the solar nebula.

Our high-precision multicollection data of hibonite, spinel, melilite, and diopside in nine CAIs from reduced CV3 chondrites Efremovka, TIL 07003, and TIL 07007 yield internal isochrons. These diagrams clearly show

significant variations in $(^{26}\text{Al}/^{27}\text{Al})_0$ value among the inclusions, ranging from $(5.59 \pm 0.25) \times 10^{-5}$ to $(2.49 \pm 0.72) \times 10^{-5}$ (**Fig. 1**).

The $(^{26}\text{Al}/^{27}\text{Al})_0$ values inferred from four FGIs (E-A-01, E-B-01, TIL 3-02, and TIL 7-06) are broadly consistent with the bulk refractory inclusion value of $\sim 5.2 \times 10^{-5}$ [5,6]. The similar value was also inferred from ten FGIs [2-4]. We interpret this clustering at $\sim 5.2 \times 10^{-5}$ as a timing of the first condensation event for FGIs when ^{26}Al became relatively homogeneous at the canonical level. In contrast, three FGIs (E-A-2, TIL 3-05, and TIL 7-02) exhibit distinctly lower $(^{26}\text{Al}/^{27}\text{Al})_0$ values than the canonical value of $\sim 5.2 \times 10^{-5}$ [5,6]. TIL 3-05 has the lowest $(^{26}\text{Al}/^{27}\text{Al})_0$ value of $(2.49 \pm 0.72) \times 10^{-5}$. [4] also reported a range of $(^{26}\text{Al}/^{27}\text{Al})_0$ values down to as low as $(3.34 \pm 0.20) \times 10^{-5}$ from five out of seven FGIs analyzed. This observed spread from FGIs suggests multiple condensation events in the early solar nebula: that is, CAI condensation continued over a time span of at least ~ 0.8 Ma after initial condensation. Moreover, two FTAs (TIL 7-01 and TIL 7-07) yield a range of $(^{26}\text{Al}/^{27}\text{Al})_0$ values down to $\sim 3.5 \times 10^{-5}$. Previously, variations in $(^{26}\text{Al}/^{27}\text{Al})_0$, ranging from $\sim 5.3 \times 10^{-5}$ down to $\sim 4.4 \times 10^{-5}$, were also inferred from FTAs [7,13,14]. This observed spread from FTAs can also reach the same interpretation that CAI condensation continued over a time span of at least ~ 0.4 Ma after initial condensation. The overall range of $(^{26}\text{Al}/^{27}\text{Al})_0$ values inferred from FGIs, FTAs, and an AOA in CV3 chondrites [2-4,7,13,14,this study] overlap with those obtained from CGIs [10], implying that CAIs were continuously produced and reprocessed in the early solar nebula. Alternatively, this range may be an indicator of heterogeneous distribution of ^{26}Al in the CAI-forming region [4,14].

A previous Al-Mg isotopic study of small FGIs

(<200 μm in size) from a pristine CO3 chondrite Allan Hills A77307 identified two prominent peaks at $(^{26}\text{Al}/^{27}\text{Al})_0 = 5.4 \times 10^{-5}$ and 4.9×10^{-5} [15]. This was interpreted that a second major thermal event occurred $\sim 10^5$ years after initial condensation. The collective data set of FGIs and FTAs from CV3 chondrites suggests that lower $(^{26}\text{Al}/^{27}\text{Al})_0$ than the canonical value become statistically important. Thus, more Al-Mg isotopic analyses are required to test if there are other peaks in the distribution of $(^{26}\text{Al}/^{27}\text{Al})_0$ that may be evidence for episodic thermal re-processing events in the nebula-wide CAI-forming region.

Conclusions: Our high-precision SIMS data obtained from FGIs and FTAs in reduced CV3 chondrites yield internal isochrons with a spread in $(^{26}\text{Al}/^{27}\text{Al})_0$ values. The observed spread in $(^{26}\text{Al}/^{27}\text{Al})_0$ values down to $\sim 2.5 \times 10^{-5}$ suggests that the CAI formation by condensation occurred repeatedly in the early solar nebula, probably over an extended period of at least ~ 0.8 Ma after initial condensation.

Acknowledgements: This study was supported by NASA grant 80NSSC21K1558 (JH) and NASA ISFM funding to the JSC Coordinated Analysis Work Package (LPK). **References:** [1] Krot A. N. et al. (2004) MAPS 39, 1517-1553. [2] MacPherson G. J. et al. (2010) ApJ 711, L117-L121. [3] MacPherson G. J. et al. (2020) MAPS 55, 2519-2538. [4] Kawasaki N. et al. (2020) GCA 2179, 1-15. [5] Jacobsen B. et al. (2008) EPSL 272, 353-364. [6] Larsen K. K. et al. (2011) ApJ 735, L37. [7] MacPherson G. J. et al. (2012) EPSL 331-332, 43-54. [8] Han J. and Brearley A. J. (2015) MAPS 50, 904-925. [9] Han J. et al. (2021) 84th MetSoc, abstract #6267. [10] MacPherson G. J. et al. (2017) GCA 201, 65-82. [11] MacPherson G. J. et al. (1984) GCA 48, 29-46. [12] Liu M.-C. et al (2018) Int J Mass Spectrom 424, 1-9. [13] MacPherson et al. (2013) 44th LPSC, abstract #1530. [14] Kawasaki N. et al. (2019) EPSL 511, 25-35. [15] Liu M.-C. et al. (2019) Sci Adv 5, eaaw3350. [16] MacPherson G. J. et al. (2018) EPSL 491, 238-243. [17] MacPherson G. J. et al. (2022) GCA 321, 343-374. [18] Kita N. T. et al. (2012) GCA 86, 37-51. [19] Kawasaki N. et al. (2018) GCA 221, 318-341. [20] Kawasaki N. et al. (2021) MAPS 56, 1224-1239. [21] MacPherson G. J. et al. (2017) GCA 201, 65-82.

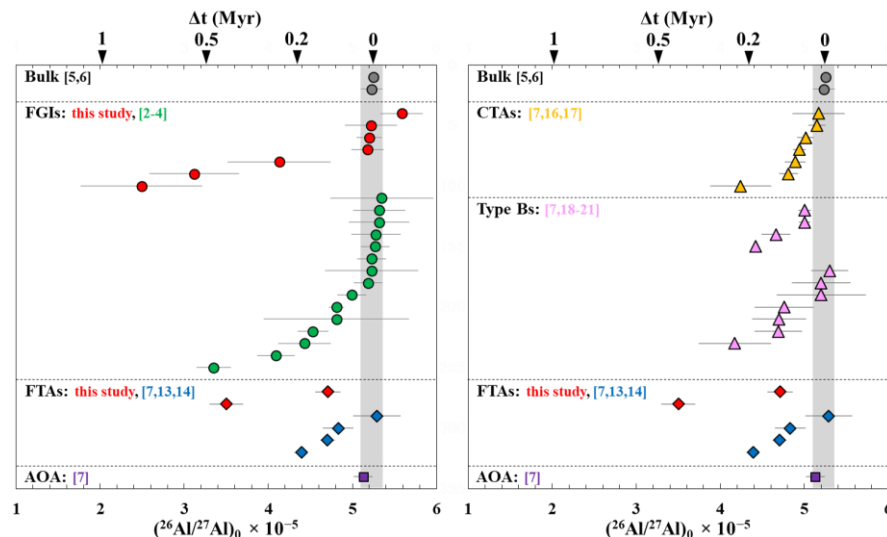


Figure 1. Comparison of inferred $(^{26}\text{Al}/^{27}\text{Al})_0$ values from different types of CV3 CAIs determined by in situ SIMS measurements.